Measurement 89 (2016) 322–327

Contents lists available at ScienceDirect

Measurement

journal homepage: www.elsevier.com/locate/measurement

Motor current signature analysis via four-channel FIR filter banks

Levent Eren [a,*], Murat Aşkar [a], Michael J. Devaney [b]

[a] Izmir University of Economics, Faculty of Engineering and Computer Science, Balcova, Izmir, Turkey
[b] University of Missouri-Columbia, College of Engineering, Columbia, MO, USA

ARTICLE INFO

Article history:
Received 6 November 2014
Received in revised form 6 April 2016
Accepted 12 April 2016
Available online 13 April 2016

Keywords:
MCSA
Wavelet packet decomposition
M-channel filter banks

ABSTRACT

Motor current signature analysis (MCSA) is capable of providing continuous monitoring of induction motors in a non-intrusive manner. Fourier based techniques have been used widely in processing of stator current but these techniques have a shortcoming in processing non-stationary signals such as the stator current. Recently, wavelet packet decomposition (WPD) has become popular in such applications since it gives better results in the case of non-stationary signals. The latter approach has much higher computational complexity limiting its use in motor diagnostics applications. In this study, the use of four-channel FIR filter banks is proposed to provide lower computational complexity. Four-channel filter banks employ higher level of parallel processing than currently used two-channel filter banks. FPGA implementation of the proposed algorithm would result in even further reduction in overall computation time.

1. Introduction

Induction motor faults can be classified into two categories: electrical and mechanical. Bearing defects, shaft misalignment, and air gap eccentricity are mechanical problems whereas broken rotor bars and winding defects are electrical ones [1,2]. Motor vibration analysis is used widely in detecting mechanical faults [2–8]. Motor current signature analysis (MCSA) provides a non-intrusive way to continuously monitor the condition of an induction motor. Scientists at Oak Ridge National Laboratory had initiated the research in this area by studying nonintrusive means for detecting the mechanical and electrical problems in both motor and driven equipment via MCSA [9]. Schoen et al. showed that the relationship of bearing vibration to the stator current spectrum can be determined by an equation based on the work for dynamic eccentricity by Kliman et al. [10,11]. Fourier based and wavelet transform based techniques are used in analysis [12–18]. Neural networks and other decision making algorithms have been applied to both motor vibration and current data to improve motor fault detection [19–34].

In this study, MCSA is performed by using four-channel FIR filters in wavelet packet decomposition [35,36]. The prototype FIR low-pass filter is designed using traditional filter design methods. Then, band-pass and high-pass filters obtained by poly-phase implementation of the prototype filter. The proposed method provides computationally more efficient way than currently used implementation of half-band filters in MCSA without a compromise in the accuracy of motor fault detection.

2. Four-channel FIR filter banks

Multi-band signal decomposition is used widely in image and voice processing applications. Wavelet transform and multirate filter banks are closely related. Multirate filter banks provide the necessary structure for generating the important cases of wavelets and the wavelet transform [37]. Multi-channel filtering can result in computationally more efficient implementation if the poly-phase decomposition is used.

Writing low-pass prototype filter $H_0(z)$ as,

$$H_0(z) = \sum_{k=-\infty}^{\infty} h_0(k) z^{-k} \tag{1}$$

If $P_r(z)$ is defined as,

$$P_r(z) = \sum_{l=-\infty}^{\infty} h_0(r + lM) z^{-l} \tag{2}$$

where $r = 0, 1, \ldots, M-1$. Then, the filter becomes

$$H_0(z) = \sum_{r=0}^{M-1} z^{-r} P_r(z^M) \tag{3}$$

* Corresponding author.
E-mail address: levent.eren@ieu.edu.tr (L. Eren).

http://dx.doi.org/10.1016/j.measurement.2016.04.025
0263-2241/

In the case of $M = 2$, the filters become half-band filters. The prototype low-pass filter H_0 is composed of two poly-phase components P_0 and P_1.

$$H_0(z) = P_0(z^2) + P_1(z^2)z^{-1} \tag{4}$$

Then, the high-pass filter H_1 is given by

$$H_1(z) = P_0(z^2) - P_1(z^2)z^{-1} \tag{5}$$

A two-channel (half-band) analysis filter bank is depicted in Fig. 1. Daubechies, Beylkin, and Vaidyanathan are some of the well-known FIR filters with a set of orthonormal, compactly supported functions [38]. The coefficients for common filters and wavelet packet decomposition algorithms are given in [39].

In the case of $M = 3$, the filters become three-band filters. The prototype low-pass filter H_0 is composed of three poly-phase components P_0, P_1, and P_2.

$$H_0(z) = P_0(z^3) + P_1(z^3)z^{-1} + P_2(z^3)z^{-2} \tag{6}$$

Here, the band-pass H_1 and high-pass H_2 filters are obtained from the poly-phase components of the prototype low-pass filter H_0.

In the case of $M = 4$, the filters become four-band filters. The prototype filter $H_0(z)$ given in Eq. (7) is made up of four poly-phase parts.

$$H_0(z) = P_0(z^4) + P_1(z^4)z^{-1} + P_2(z^4)z^{-2} + P_3(z^4)z^{-3} \tag{7}$$

The poly-phase parts P_0, P_1, P_2, and P_3 of the prototype low-pass filter H_0 are then used to obtain H_1, H_2, and H_3 by Eqs. (8)–(10).

$$H_1(z) = P_0(z^4) + jP_1(z^4)z^{-1} - P_2(z^4)z^{-2} - jP_3(z^4)z^{-3} \tag{8}$$

$$H_2(z) = P_0(z^4) - P_1(z^4)z^{-1} + P_2(z^4)z^{-2} - P_3(z^4)z^{-3} \tag{9}$$

$$H_3(z) = P_0(z^4) - jP_1(z^4)z^{-1} - P_2(z^4)z^{-2} + jP_3(z^4)z^{-3} \tag{10}$$

Typical four-channel analysis filter bank is depicted in Fig. 2 where H_0 is a low-pass, H_1 and H_2 are band-pass, and H_3 is a high-pass filters respectively.

The poly-phase implementation of a four-channel filter bank is displayed in Fig. 3.

The prototype low-pass filter with fifty-six coefficients is obtained in matlab using Parks–McClellan optimal equiripple FIR filter design function. The cut-off frequency is set at quarter of bandwidth for the prototype filter. The magnitude response of the prototype low-pass filter is depicted in Fig. 4.

The prototype filter is chosen such that the transition bandwidth exhibits similar characteristics to Daubechies (db9), Beylkin and Vaidyanathan filters. The magnitude responses of four filters obtained from the prototype filter is shown in Fig. 5.

3. Motor fault frequencies

Commonly used equations for calculating characteristic vibration [5] and current frequencies [10] are given below. Outer race defect frequency, f_{OD}, the ball passing frequency on the outer race, is given by

$$f_{OD} = \frac{n}{2} f_{rm}\left(1 - \frac{\mathrm{BD}}{\mathrm{PD}}\cos\theta\right) \tag{11}$$

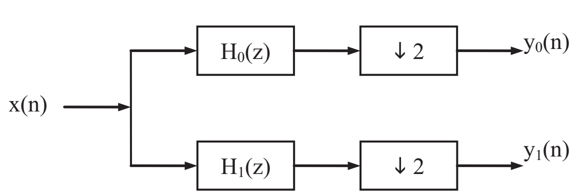

Fig. 1. Two-channel (half-band) analysis filter bank.

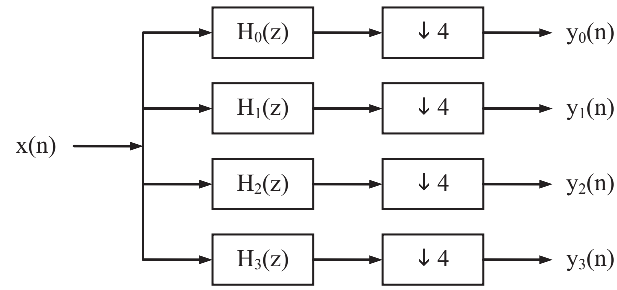

Fig. 2. Four-channel analysis filter bank.

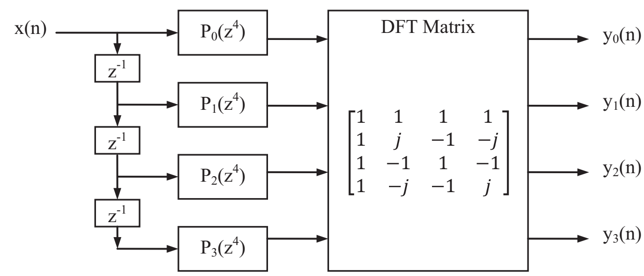

Fig. 3. Poly-phase implementation of four-channel filter bank.

where f_{rm} is the rotor speed in revolutions per second, n is the number of balls, BD is the ball diameter, and PD is the pitch diameter. The angle θ is the contact angle and is zero for ball bearings.

Inner race defect frequency f_{ID}, the ball passing frequency on the inner race, is given by

$$f_{ID} = \frac{n}{2} f_{rm}\left(1 + \frac{BD}{PD}\cos\theta\right) \tag{12}$$

Cage defect frequency f_{CD}, caused by irregularity in the train, is given by

$$f_{CD} = \frac{1}{2} f_{rm}\left(1 - \frac{BD}{PD}\cos\theta\right) \tag{13}$$

The bearing dimension data can usually be obtained from the manufacturer. The mechanical vibration due to the bearing defect results in air gap eccentricity. Oscillations in air gap width in turn cause variations in flux density. The variations in flux density affect the machine inductances producing stator current vibrational harmonics. The characteristic current frequencies, f_{CF}, due to bearing characteristic vibration frequencies are calculated by [10]

$$f_{CF} = |f_e \pm m f_v| \tag{14}$$

where f_e is the line frequency, m is an integer and f_v is characteristic vibration frequency obtained from Eqs. (11)–(13).

4. Testing and evaluation

In this part, the proposed method is tested by analyses of both simulated and real data. In the first part, the performance of the proposed four-band filter is compared with the performances of Daubechies (db9), Beylkin, and Vaidyanathan filters with simulated data. The simulations are based on the relationship of bearing vibration in Eq. (13) to the motor current defined in Eq. (14). Here, the cage defect vibration fundamental frequency is calculated to be 11.6 Hz at running speed of 1750 r/min using Eq. (13). Then, the fundamental line current (60 Hz) is modulated by the characteristic vibration fundamental frequency resulting in sidebands at 48.4 Hz and 71.6 Hz in the current spectrum. The magnitude of